RSC Advances

ROYAL SOCIETY OF CHEMISTRY

www.rsc.org/advances

ARTICLE TYPE www.rsc.org/xxxxxx | XXXXXXXX

Thermal Property and Aggregation-Induced Emission Fluorophore That Forms Metal–Ligand Complexes with $Zn(ClO_4)_2$ of Salicylaldehyde Azine–Functionalized Polybenzoxazine

Mohamed Gamal Mohamed,[a] Ruey-Chorng Lin,[a] Jia-Huei Tu,[a] Fang-Hsien Lu,[a] Jin-Long Hong,[a] Kwang-Un Jeong,[c] Chih-Feng Wang,[d] and Shiao-Wei Kuo[a,b,*]

Received (in XXX, XXX) Xth XXXXXXXXX 200X, Accepted Xth XXXXXXXXX 200X
First published on the web Xth XXXXXXXXX 200X
DOI: 10.1039/b000000x

In this report, we designed a new and simple salicylaldehyde azine–functionalized benzoxazine (Azine-BZ) monomer via Mannich condensation reaction of aniline and paraformaldehyde with 1,2-bis(2,4-dihydroxybenzylidene)hydrazine in 1,4-dioxane. Compared with 3-phenyl-3,4-dihydro-2*H*-benzooxazine monomer (263 °C), the maximum exothermic peak of Azine-BZ was shifted to a lower temperature (213 °C) based on differential scanning calorimetry (DSC) analyses because of the basicity of the phenolic group (OH) in the ortho position and the azine groups. Blending Azine-BZ with different weight ratios of zinc perchlorate [$Zn(ClO_4)_2$] to form benzoxazine/zinc ion complexes not only afflicted the thermal properties based on thermogravimetric analysis (TGA) due to physical crosslinking through metal–ligand interactions, but also expedite ring-opening polymerization, decreasing the curing temperature from 213 to 184 °C (at 10 wt% Zn^{2+}). Based on the fluorescence results, the Azine-BZ and AZine-BZ/$Zn(ClO_4)_2$ complexes were non-emissive in THF solution. Their fluorescence increased gradually upon on the addition of water contents as poor solvent. Interestingly, both the pure Azine-BZ and blending wotj $Zn(ClO_4)_2$ still emitted light after thermal curing at 150 °C, as determined through photoluminescence measurements, indicating that the azine group could act as a probe of the curing behavior of the benzoxazine monomer, as well as a fluorescent chemosensor for Zn^{2+} and, possibly, other transition metal ions through a metal–ligand charge transfer mechanism.

Introduction

Benzoxazine monomer is a molecule where it contains on an oxazine ring (a heterocyclic six-membered ring with oxygen and nitrogen atoms) is connected to a benzene ring. The last few decades, polybenzoxazine (PBZs) is a class of thermosetting resins which have been attracted widely due to their specific potential applications as phenolic resins materials.[1-3] Polybenzoxazines (PBZs) produces from the thermal curing of oxazine ring in benzoxazine monomer without any catalyst, affording to highly dense cross-linked network materials with strongly intra and intermolecular hydrogen bonding between phenolic groups and tertiary amine in Mannich linkage after ring-opening polymerization.[4] Many literatures reported that the potential applications of polybenzoxazines in industrial field, due to their unique characteristics such as, flame resistance, low surface energies, high thermal and mechanical stabilities, and low water adsorption.[5,6]

BZs are versatile thermoset resins synthesized through Mannich condensation between an aromatic phenol, a primary amine, and formaldehyde.[7-12] Nowadays, these phenolic resins can be used as thermoset to prepare polymer nanocomposites due to their unique excellent thermal properties.[13-16] The polybenozoxazine chemistry offers flexibility of many molecular designs, thereby facilitating the preparation of different PBZ nanocomposites. To control the properties of PBZs, several derivatives functionalized with reactive groups (e.g., propargyl, nitrile, alkyl, carboxyl, hydroxyalkyl) have been synthesized.[17-20] Two types of BZ-based composites have been developed: fiber-reinforced PBZ composites and inorganic particle–reinforced PBZ composites (e.g., silica, TiO_2, magnetic nanoparticles).[21]

Most fluorescing materials weaken the emissive properties, when they aggregated in a poor solvent or in the solid state. This phenomenon, known as aggregation-caused quenching (ACQ),[22,23] greatly decreased the applicability of such materials as organic light-emitting materials or fluorescent chemosensors.[24-26] At the beginning of this century, Tang et al. reported that many materials can be emitted light when dispersed in a poor solvent or fabricated into film in nano-aggregate state, these interesting phenomenon, namely as aggregation-induced emission (AIE) or aggregation-induced enhanced emission (AIEE).[27-28] AIE fluorescent materials become very strongly emissive in aggregate or solid state, but become very strongly emitters when aggregated as powders or nano-aggregates. There are many mechanisms behind AIE include restricted intramolecular rotation (RIR),[29,30] twisting intramolecular charge transfer (TICT)[31] and planarity and rotation ability.[32] Tang et al. also reported that a series of salicylaldehyde azine derivatives exhibited AIE characteristics in good solvents, but displayed very weak emissions while being strongly luminescent in poor solvents.[33] Several fluorescent chemosensors reported have been designed based on the mechanisms of photoinduced electron transfer (PET)[34], fluorescence resonance intramolecular charge transfer (FRICT)[35], and metal–ligand charge transfer (MLCT)[36], respectively. Tain et al. reported that Schiff base–modified triphenylaminobenzimidazole and pyridinecarboxaldehyde derivatives displaying AIEE characteristics acted as chemosensors for Cu(II) and Zn(II) ions.[37]

As a result, in this article we synthesized a new BZ monomer containing a salicylaldehyde azine unit (Azine-BZ)

[a]Department of Materials and Optoelectronic Science, Centerfor Functional Polymers and Supramolecular Materials, National Sun Yat-Sen University, Kaohsiung, Taiwan
E-mail: kuosw@faculty.nsysu.edu.tw
[b]Department of Medicinal and Applied Chemistry, Kaohsiung Medical University, Kaohsiung, Taiwan.
[c]Department of Polymer-Nano Science and Technology, Chonbuk National University, Jeonju, Korea
[d]Department of Materials Science and Engineering, I-Shou University, Kaohsiung, Taiwan

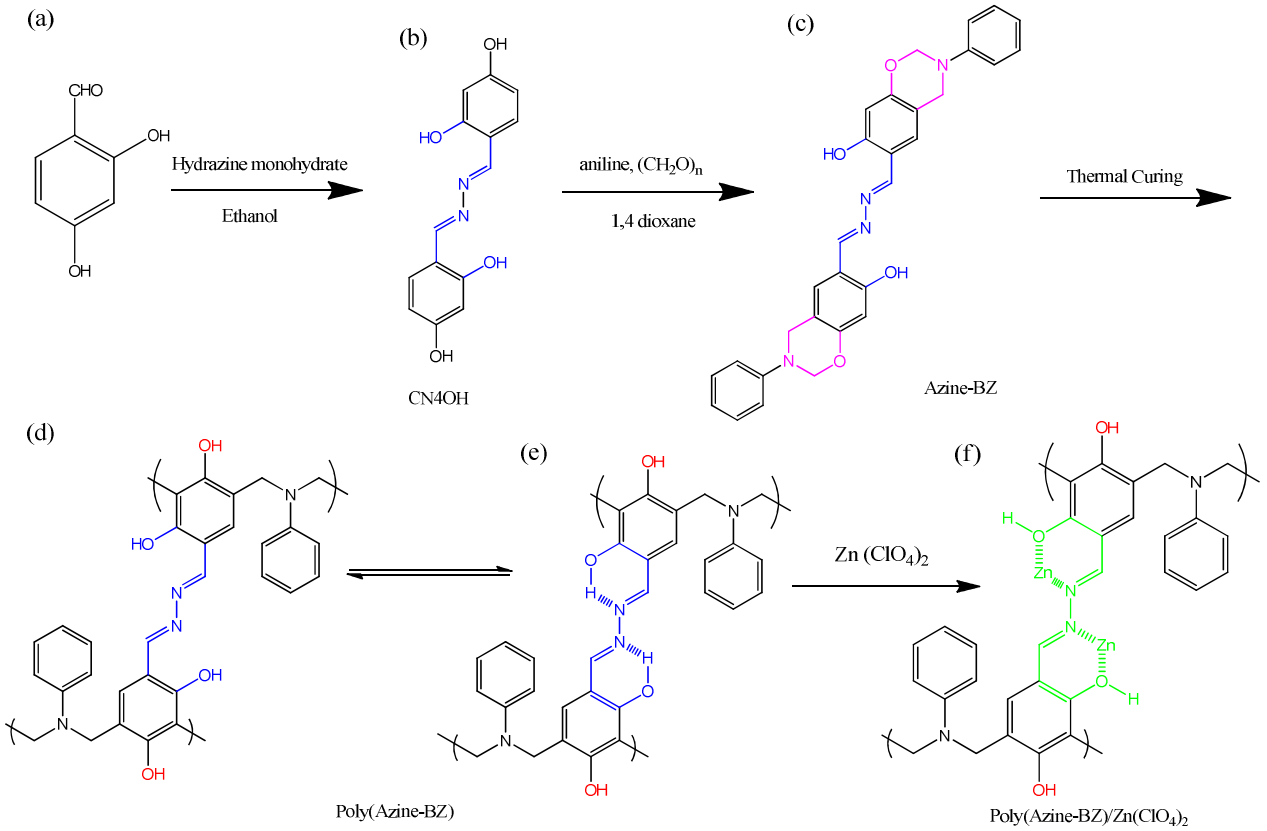

Scheme 1: Synthesis and chemical structures of (a) 2,4-dihydroxybenzaldehyde, (b) CN4OH, (c) Azine-BZ, (d, e) poly(Azine-BZ), and (f) the poly(Azine-BZ)/Zn$(ClO_4)_2$ complex.

through facile and simple Mannich condensation reaction of 1,2-bis(2,4-dihydroxybenzylidene)hydrazine (CN4OH), paraformaldehyde, and aniline in the presence 1,4-dioxane as good solvent (Scheme 1). We also studied the thermal curing polymerization, thermal stabilities, the absorption and emission behavior, specific metal-ligand interaction when Azine-BZ blended with various weight ratios of zinc perchlorate [$Zn(ClO_4)_2$], before and after thermal curing via chelation complexes by using differential scanning calorimetry (DSC), Fourier transform infrared (FTIR) spectroscopy, thermogravimetric analysis (TGA), UV-Vis and photoluminescence (PL) spectroscopy. In addition, we used transmission electron microscopy (TEM) and dynamic light scattering (DLS) to characterize the self-assembled nano-aggregates morphology which formed from the Azine-BZ monomer in THF/water solvent pairs.

Experimental Section

Materials

Paraformaldehyde (96%), aniline, 2,4-Dihydroxybenzaldehyde were used as received from Acros. Ethyl acetate (EA), hydrazine monohydrate (98%), chloroform, dichloromethane, ethanol, tetrahydrofuran (THF), and 1,4-dioxane were used as received from Scharlau. Zinc perchlorate hexahydrate [$Zn(ClO_4)_2 \cdot 6H_2O$] was purchased from Aldrich and dried overnight in a vacuum oven at 70 °C to remove water.

Bis(2,4-dihydroxybenzylidene)hydrazine (CN4OH)[33,38]

Under a N_2 atmosphere in a 150-mL two-neck round-bottom flask equipped with a stirrer bar, hydrazine monohydrate (0.900 g, 18.1 mmol), 2,4-dihydroxybenzaldehyde (5.00 g, 36.2 mmol) were dissolved in absolute EtOH (100 mL) After stirring overnight at room temperature, the precipitate was filtered off and washed three times with EtOH. The yellow powder was recrystallized from a small amount of THF, affording yellow crystals (8.50 g, 86%); FTIR (KBr, cm^{-1}): 3200–3400 (OH stretching). ^1H NMR (500 MHz, DMSO-d_6, δ, ppm): 11.94 (s, 1H, OH_a), 10.10 (s, 1H, OH_b), 8.75 (d, 2H, H_c), 7.36 (t, 2H, H_d), 7.04 (d, 1H, H_e), 6.96 (t, 1H, H_f). ^{13}C NMR (125 MHz, DMSO-d_6, δ, ppm): 162.9, 162.6, 161.5, 133.6, 110.8, 110.8, 108.8, 103.1. High resolution FT-MS (m/z) for MH^+ ($C_{14}H_{12}N_2O_4$): 273.09: calc.: 272.08 (Figure S2).

Synthesis of Azine-BZ[39]

50 mL of 1,4-dioxane/ethanol, paraformaldehyde (0.882 g, 29.4 mmol), 1,2-bis(2,4-dihydroxybenzylidene)hydrazine CN4OH (2.00 g, 7.35 mmol), and aniline (1.37 g, 14.7 mmol) were mixed in a 150-mL two-neck round-bottom flask under a N_2 atmosphere with a reflux condenser. The reaction solution was heated under reflux for 18 h at 90–110 °C. After that, cooling the reaction mixture to room temperature, the solvent was evaporated under reduced pressure to give a yellow solid, which was purified through column chromatography (SiO_2; EtOAc) to give a yellow solid (3.21 g, 87%). FTIR (KBr, cm^{-1}): 3300–3200 (OH stretching), 931 and 1488 (vibrations of trisubstituted benzene ring). ^1H NMR (500 MHz, $CDCl_3$, δ, ppm): 11.93 (s, 1H, H_a), 8.71 (s, 1H, H_b), 4.70 (s, 2H, Ar-CH_2-N), 5.33 (s, 2H, O-CH_2-N), 6.92–8.43 (m, CH aromatic). ^{13}C NMR (125 MHz, $CDCl_3$, δ, ppm): 45.93 (CCH_2N), 80.04 (OCH_2N). High resolution FT-MS (m/z) for MH^+ ($C_{14}H_{12}N_2O_4$): 507.20: calc.: 506.20 (Figure S3).

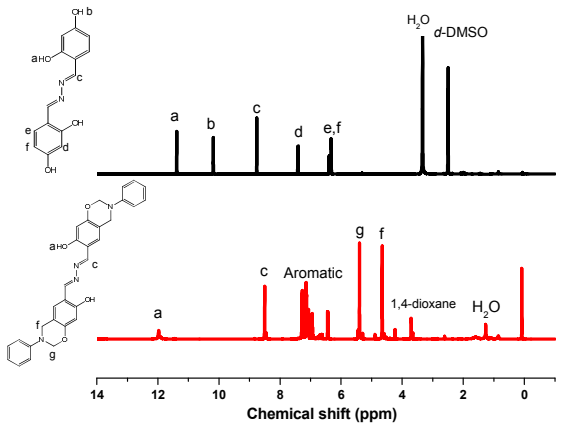

Figure 1: ^{1}H NMR spectra of (a) CN4OH and (b) Azine-BZ

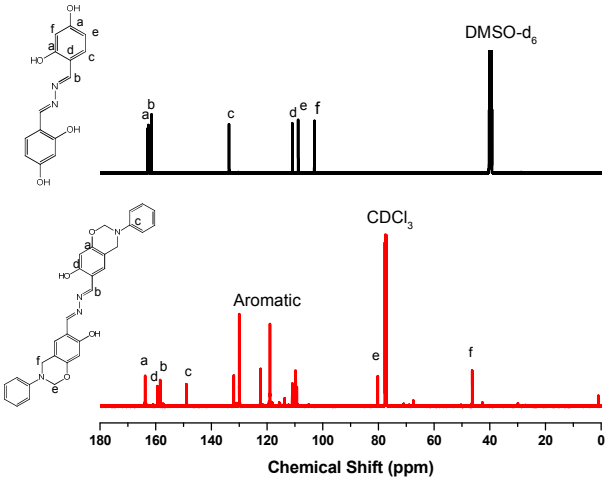

Figure 2: ^{13}C NMR spectra of (a) CN4OH and (b) Azine-BZ

Poly(Azine-BZ)/Zinc Complexes

$Zn(ClO_4)_2$ (1, 2, 3, 4, 5, or 10 wt%) was dissolved in 5 mL of THF 1 h. Then, $Zn(ClO_4)_2$ solutions were added dropwise to Azine-Bz solutions. After that, the Azine-Bz/$Zn(ClO_4)_2$ complexes solutions were stirred for 2 days, the removal of solvent under reduced pressure. Each blended mixture was poured into a stainless- mold and polymerized in a stepwise manner, with heating at 110, 150, 180, 210, and 240 °C for 2 h at each temperature. The color of each cured sample was dark red.

Nanoaggregates of Azine-BZ and Azine-BZ/Zinc Complexes

Stock solutions of Azine-BZ and Azine-BZ/Zinc were prepared in THF at 100-mL volumetric flask with concentrations of 1 × 10^{-4} M. Then, water (poor solvent) was added dropwise under vigorous stirring to prepare different volume ratios (0–90%) was reached. PL spectra of the suspension of nano-aggregates were recorded immediately.

Characterization

Nuclear magnetic resonance (^{1}H and ^{13}C NMR) spectra were recorded on an INOVA 500 by using DMSO-d_6 and $CDCl_3$ as solvents. Fourier transform infrared (FTIR) spectra of the KBr disks of CN4OH and Azine-BZ were measured by a Bruker Tensor 27 FTIR spectrophotometer and thirty-two scans were collected at a spectral resolution of 4 cm^{-1}. Differential scanning calorimeter (DSC) measurements were conducted with TA Q-20 with operated under a N_2 as purge gas (50 mL/min) at heating rate of 20 °C/min. The sample (ca. 3-5 mg) was placed in a sealed aluminum sample pan. Dynamic curing scans were recorded from 30 to 350 °C at a heating rate of 20 °C min^{-1}. The thermal stabilities of the samples were measured using a TA Q-50 thermogravimetric analyzer operated under a N_2 as purge gas (60 mL/min) at heating rate of 20 °C/min from 30 to 800 °C under UV–Vis spectra were recorded using a Shimadzu mini 1240 spectrophotometer; the concentration of Azine-BZ in THF was 10^{-4} M. Photoluminescence spectra was collected at room temperature using a monochromatized Xe light source. Particle sizes of the aggregates in solution were measured by DLS using a Brookhaven 90 plus spectrometer equipped with a temperature controller. Argon into laser operating at 658 nm was used as the light source. TEM images were recorded using a JEOL-2100 transmission electron microscope operated at an accelerating voltage of 200 kV. The molecular weights of CN4OH and Azine-BZ were recorded using a Bruker Solarix high resolution Fourier Transform Mass spectroscopy system FT-MS (Bruker, Bremen, Germany).

Results and Discussion

Synthesis and Characterization of CN4OH and Azine-BZ

Scheme 1 displays our synthesis of the salicylaldehyde azine–functionalized BZ monomer (Azine-BZ). First, we employed a Schiff base condensation of 2,4-dihydroxybenzaldehyde with hydrazine monohydrate in EtOH to obtain CN4OH; we then prepared Azine-BZ with high purity more than 95% in through a Mannich condensation reaction of CN4OH, paraformaldehyde, and aniline in 1,4-dioxane at 80-90 °C. We carefully confirmed the chemical structures of CN4OH and Azine-BZ via ^{1}H NMR, ^{13}C NMR, and FTIR spectroscopy. Figure 1 illustrated the ^{1}H NMR spectra of CN4OH and Azine-BZ. The spectrum of CN4OH [Figure 1(a)] features signals at 10.10 and 11.94 ppm, representing the OH groups of the phenolic units, as well as signals in the range 6.33–7.40 ppm for the aromatic protons and at 8.69 ppm for the N=CH groups. The spectrum of the AIE unit (azine)–based BZ monomer [Figure 1(b)] lacked the peak at 10.10 ppm for the OH_b proton of CN4OH, but featured peaks at 6.36–7.26 ppm for the aromatic protons and resonances at 4.70 ($ArCH_2N$) and 5.33 (OCH_2N) ppm at a 1:1 ratio; no signal was present near 4.0 ppm, corresponding to an NCH_2Ph unit, as a result of ring opening of the BZ moiety; no other major peaks were evident in the ^{1}H NMR spectrum, indicating that Azine-BZ had successfully formed. Figure 2 presents the ^{13}C NMR spectra of CN4OH and Azine-BZ. The spectrum of CN4OH [Figure 2(a)] features signals for the carbon nuclei in the aromatic rings and double bonds in the range 103.77–163.27 ppm. The spectrum of Azine-BZ [Figure 2(b)] displays characteristic resonances for the $ArCH_2N$ and OCH_2N units of the oxazine ring at 45.93 and 80.05 ppm, respectively. Figure S1 presents the FTIR spectra of CN4OH and Azine-BZ, recorded at room temperature. The spectrum of CN4OH [Figure S1(a)] features three sharp peaks at 3217, 3481, and 3522 cm^{-1} for the intra and intermolecular hydrogen-bonded and free OH groups, and sharp signals for the aromatic rings at 831, 1599, 1619, and 3033 cm^{-1}. The spectrum of Azine-BZ [Figure S1(b)] features characteristic absorption bands at 1366 (tetrasubstituted benzene ring), 1225 (asymmetric COC stretching), 1042 (symmetric COC stretching), and 931 (stretching vibrations of oxazine ring) cm^{-1}.

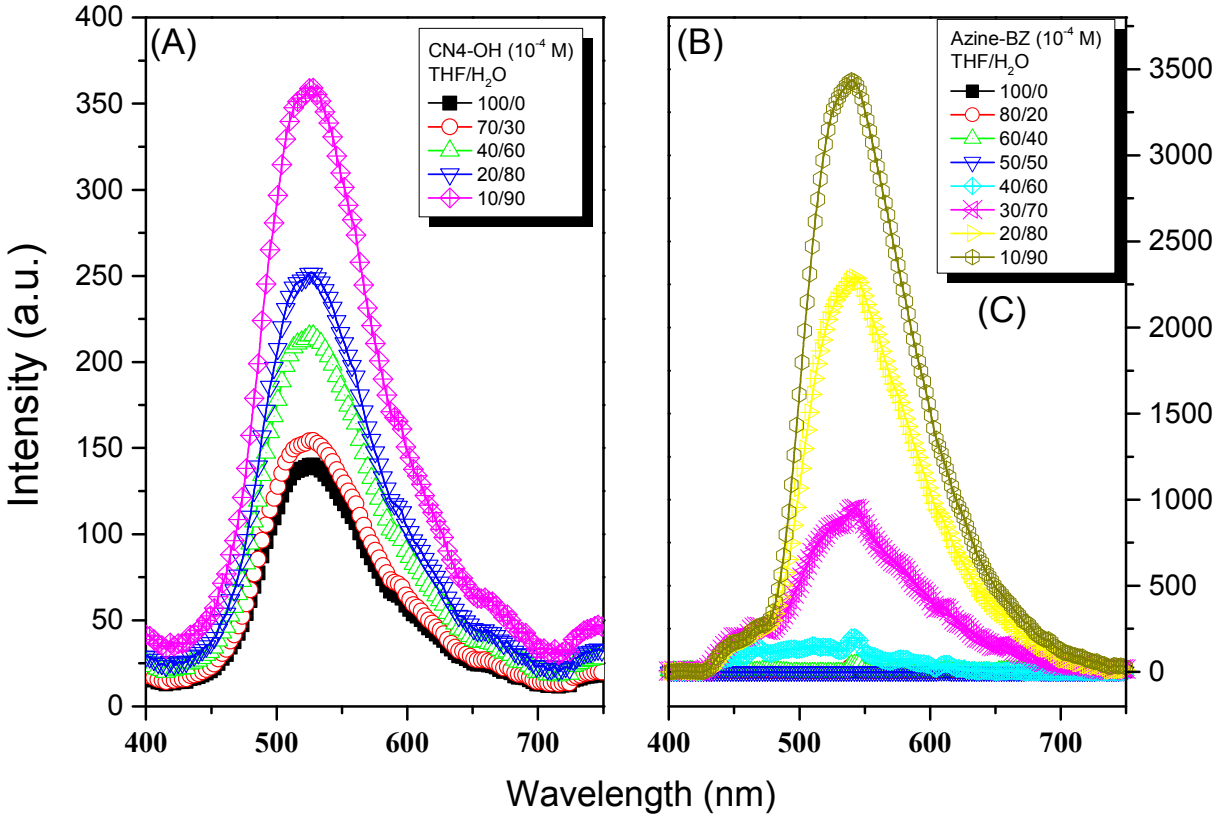

Figure 3: (A, B) PL spectral changes of (A) CN4OH and (B) Azine-BZ (1.0×10^{-4} mol L^{-1}) and (C) PL intensity of Azine-BZ in THF/water mixtures at various water fractions.

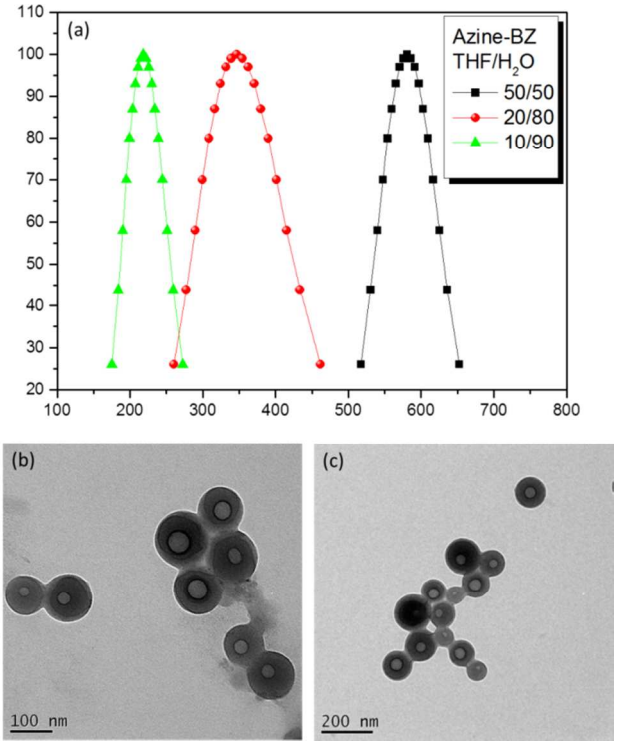

Figure 4: (a) Particle size distributions of Azine-BZ in THF/water mixtures at water fractions of 50, 80, and 90%. (b, c) TEM images of Azine-BZ at a concentration of 1.0×10^{-4} mol L^{-1} in THF/water mixtures at ratios of (b) 20:80 and (c) 10:90 (v/v)

High resolution FT-MS displayed the exactly molecular weights of CN4OH and Azine-BZ, respectively (supporting information Figure S2 and S3). Combined these spectral data are consistent with the successful synthesis of a new Azine-BZ monomer.

Optical Properties and AIE of CN4OH and Azine-BZ

The UV–Vis absorption spectrum of Azine-BZ monomer in THF (1×10^{-4} M) features (Figure S4) an absorption peak at 370 nm that we attribute to the π–π* transition of the salicylaldehyde azine unit. Most reported salicylaldehyde azine are fluorescent AIE materials and it can emit different light in their aggregated states, presumably because of RIR and excited state intramolecular proton transfer [ESIPT].[33,38] We investigated the AIE phenomena of CN4OH and Azine-BZ in THF/H_2O mixtures at water contents in the range 0–90%. CN4OH and Azine-BZ are both soluble in common organic solvents (THF, DMSO, DMF), but insoluble in water and hexane. As expected, solutions of CN4OH and Azine-BZ in THF are virtually non-luminescent, as determined from their fluorescence spectra [Figures 3(A) and 3(B)]. The fluorescence intensities increased gradually, however, when the water content was greater than 80% for CN4OH and 90% for Azine-BZ [Figure 3(C)], with the emissions of CN4OH and Azine-BZ turning on and displaying green fluorescence. These emissions from CN4OH and Azine-BZ were presumably induced through aggregate formation, suggesting that both CN4OH and Azine-BZ exhibit AIE. In addition, we found that Azine-BZ could form nanoparticles in solution; we used transmission electron microscopy (TEM) and dynamic light scattering (DLS) to

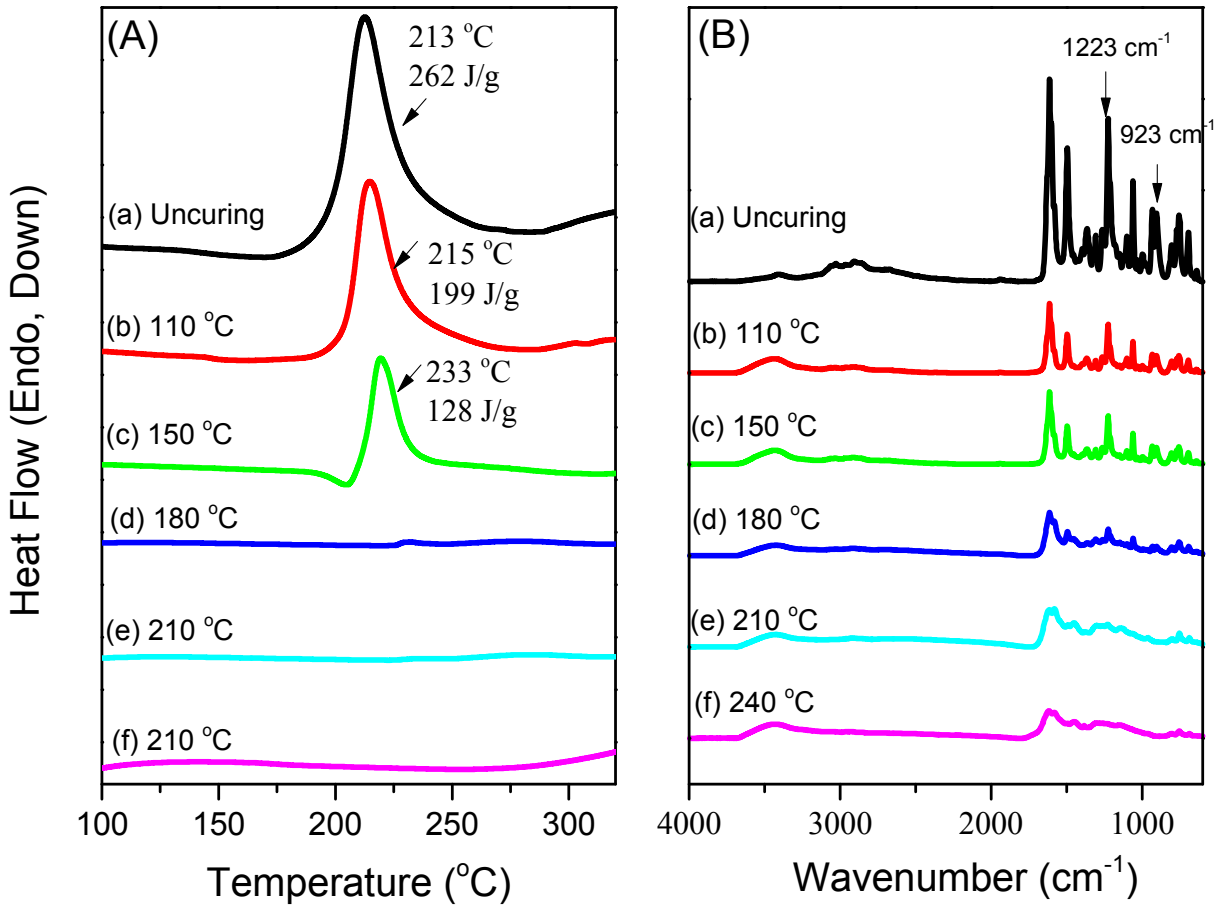

Figure 5: (A) DSC profile and (B) FTIR spectra of Azine-BZ monomer recorded after thermal treatments

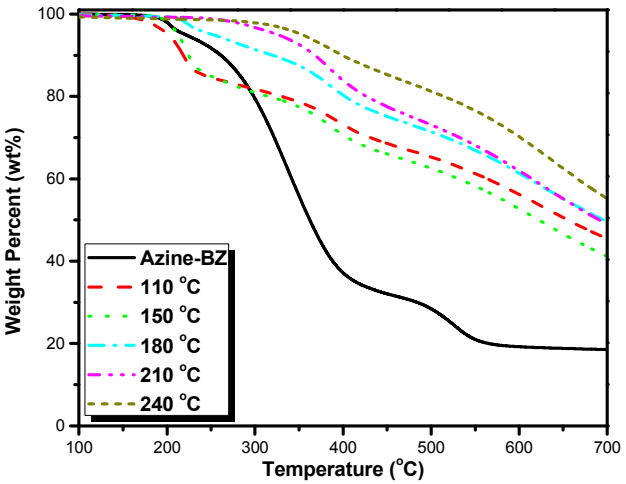

Figure 6: Thermogravimetric analyses of Azine-BZ monomer, recorded after thermal polymerization at 110, 150, 180, 210 and 240 °C

investigate the growth of these nano-aggregates at high water contents 90% (Figure 4). The TEM images in Figures 4(b) and 4(c) reveal nano-aggregates having sizes of approximately 100–200 nm, consistent with the DLS data. The particle sizes decreased upon increasing the water content, reaching approximately 215 nm when the water content was 90 wt% [Figure 4(a)]. The particle sizes determined from the TEM images were smaller than those measured using DLS, because evaporation was necessary to prepare the samples for TEM, unavoidably leading to collapse and shrinkage of the particles. We suspect that CN4OH and Azine-BZ emitted intensely in their aggregated states because the large amount of water leads to form spherical nano-aggregated structures thereby restricted intramolecular rotation of the phenyl rings rotors of CN4OH and Azine-BZ.

Thermal Curing and AIE of Azine-BZ

Differential scanning calorimetry (DSC) is a convenient and simple method to understand and investigate the study the thermal curing and ring-opening polymerization of the Azine-BZ monomer. The DSC thermograms of the pure Azine-BZ monomer, recorded at a heating rate of 20 °C min^{-1} from 20 to 350 °C, reveal [Figure 5(A)] an exothermic peak with the curing temperature at 213 °C and a reaction heat of 262 J g^{-1}. Based on DSC profile the polymerization exotherm maximum temperature for Azine-BZ (213 °C) was lower than that (263 °C) for conventional 3-phenyl-3,4-dihydro-2*H*-benzooxazine (Pa-type)[1], presumably because the basic azine group in the backbone structure catalyzed the ring-opening polymerization. Clearly, after thermal treatment at 180 and 240 °C for 2 h at each temperature of Azine-BZ, the maximum exothermic peak completely disappeared which indicating the completion of ring-opening polymerization of Azine-BZ. We also studied the thermal polymerization of Azine-BZ at elevated temperatures in Figure 5(B). As shown in Figure 5(B) displays that the

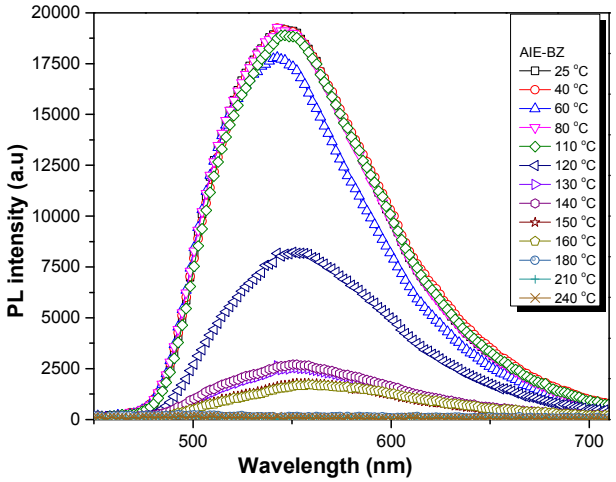

Figure 7: PL spectra of Azine-BZ monomer in the bulk state, recorded after each curing stage

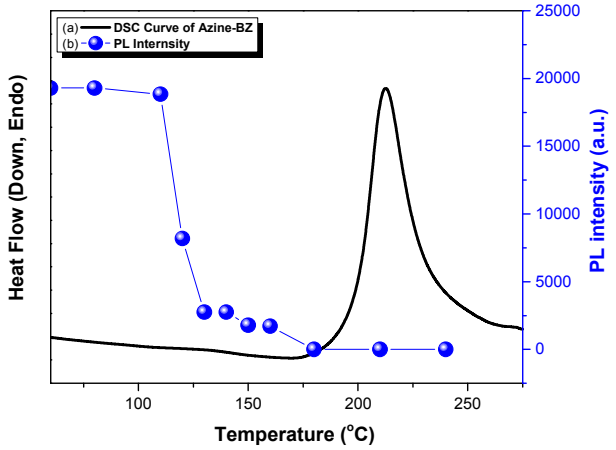

Figure 8: (a) DSC scan and (b) PL intensity of pure Azine-BZ monomer after each thermal curing stag

intensities of the characteristic absorption bands of antisymmetric COC and out-of-plane of benzene mode with attached to benzene ring gradually disappeared after thermal curing at 180 °C, corresponding to ring-opening of benzoxazine monomer and formation of Poly(Azine-BZ). In addition, a new absorption signal appearing at 3433 cm^{-1}, was corresponding to the released OH group, consistent with the DSC analyses.

Thermal stability of Azine-BZ has been investigated by thermogravimetric analysis as shown in Figure 6 after various thermal treatments. Our TGA analysis revealed (Figure 6) that the initial thermal decomposition temperature (T_{d5}) was strongly dependent on the curing exothermic peak in the DSC analysis [Figure 5(A)]. For example, the initial thermal decomposition temperatures were near 215 and 233 °C when the curing temperatures were 110 and 150 °C, respectively; these values are close to the curing exothermic peaks in the DSC analyses in Figure 5(A). In addition, the value of T_{d5} and the char yield both increased upon increasing the curing temperature. When the curing temperature was 240 °C, the value of T_{d5} increased significantly to 340 °C and the char yield was approximately 55 wt%. This char yield is higher than that of conventional 3-phenyl-3,4-dihydro-2*H*-benzooxazine (ca. 48 wt%) at 700 °C, indicating a more highly cross-linked structure arising from the presence of the azine groups, as well as from

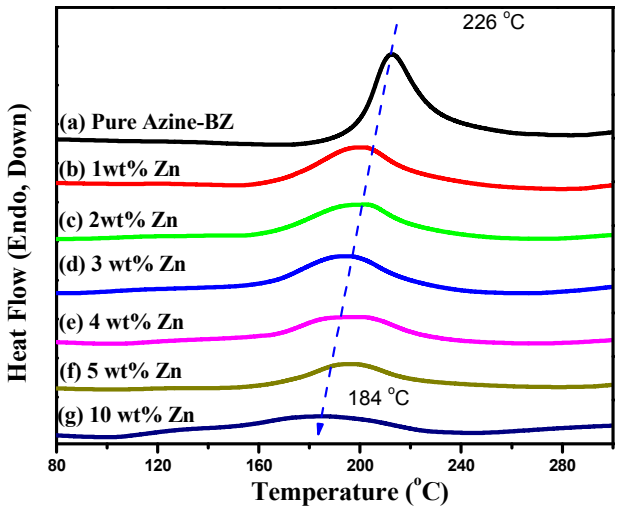

Figure 9: DSC thermograms of Azine-BZ in the presence of various weight ratios of $Zn(ClO_4)$

intramolecular hydrogen bonding involving the azine groups [Scheme 1(d)]. Figure 7 presents the PL spectra of pure Azine-BZ recorded after thermal curing at various temperatures. The maximum intensity emission of the uncured Azine-BZ was higher than those after curing. Interestingly, Azine-BZ still emitted light after curing at 150 °C. The ^{1}H NMR spectrum of Azine-BZ after thermal curing at 150 °C indicated that ring-opening polymerization had not occurred: the two peaks at 4.70 and 5.33 ppm representing the oxazine ring were still present [Figure S5(b)]. The emission was quenched after curing at 180, 210, and 240 °C. As a result, the emission from the azine could also be used as a probe of the extent of curing of the BZ monomer. Figure 8 summarizes the PL intensity of pure Azine-BZ after each curing and DSC thermal scan. The emission intensity was quenched after curing at 180 °C [Figure 8(b)], consistent with the initial thermal curing based on DSC analysis [Figure 8(a)]. In addition, the characteristic absorption bands at 923 cm^{-1} disappeared completely after curing at 180 °C [Figure 5(B)]. To the best of our knowledge, this report provides the first example of emission behavior being used to monitor curing behavior in a manner consistent with DSC and FTIR spectroscopic data.

AIE Phenomena and Thermal Polymerization of Azine-BZ/$Zn(ClO_4)_2$ Complexes

The thermal uncuring behavior of Azine-BZ/$Zn(ClO_4)_2$ complexes was investigated using DSC and FTIR, respectively. Figure 9 reveals that the thermal curing peaks shifted to lower temperature upon increasing the $Zn(ClO_4)_2$ content, decreasing from 213 °C initially to 184 °C in the presence of 10 wt% $Zn(ClO_4)_2$, suggesting that the Zn^{2+} ions enhanced the ring opening process.[39-41] FTIR analyses was carried out to investigate the specific interaction (metal-ligand interaction) of Azine-BZ after blended with various $Zn(ClO_4)_2$ contents at ambient temperature and the spectra displayed in Figure 10. Analysis of these spectra suggests that the shifts observed in the absorption peaks of the polymer structures were caused by specific ion–dipole interactions. Concentrating on the azine band at 1632 cm^{-1}, we assign the new band at 1664 cm^{-1} that appeared at 5 or 10 wt% $Zn(ClO_4)_2$ to the azine groups coordinating as π-bonding ligands to zinc cations (inset to Figure 10). Therefore, the higher energy of this new absorption was the result of formation of such a metal-ligand complex.

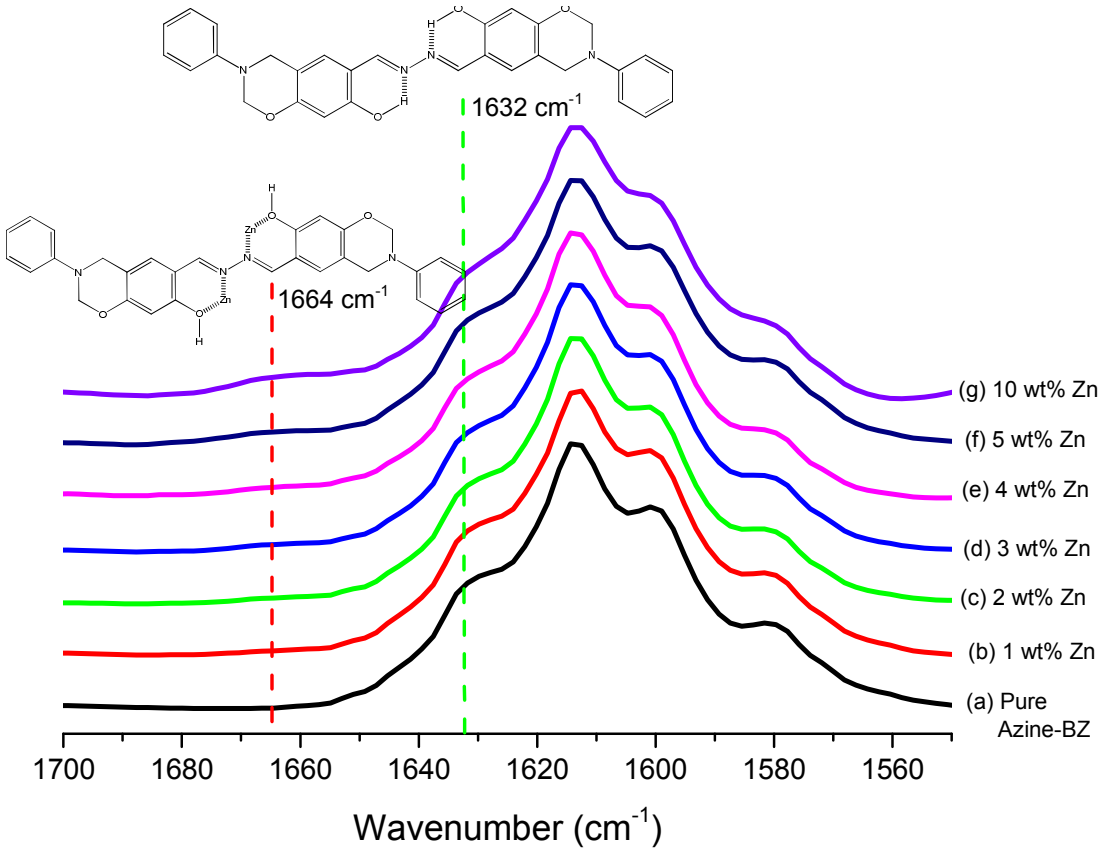

Figure 10: FTIR spectra of Azine-BZ in the presence of various amounts of $Zn(ClO_4)_2$, recorded at ambient temperature

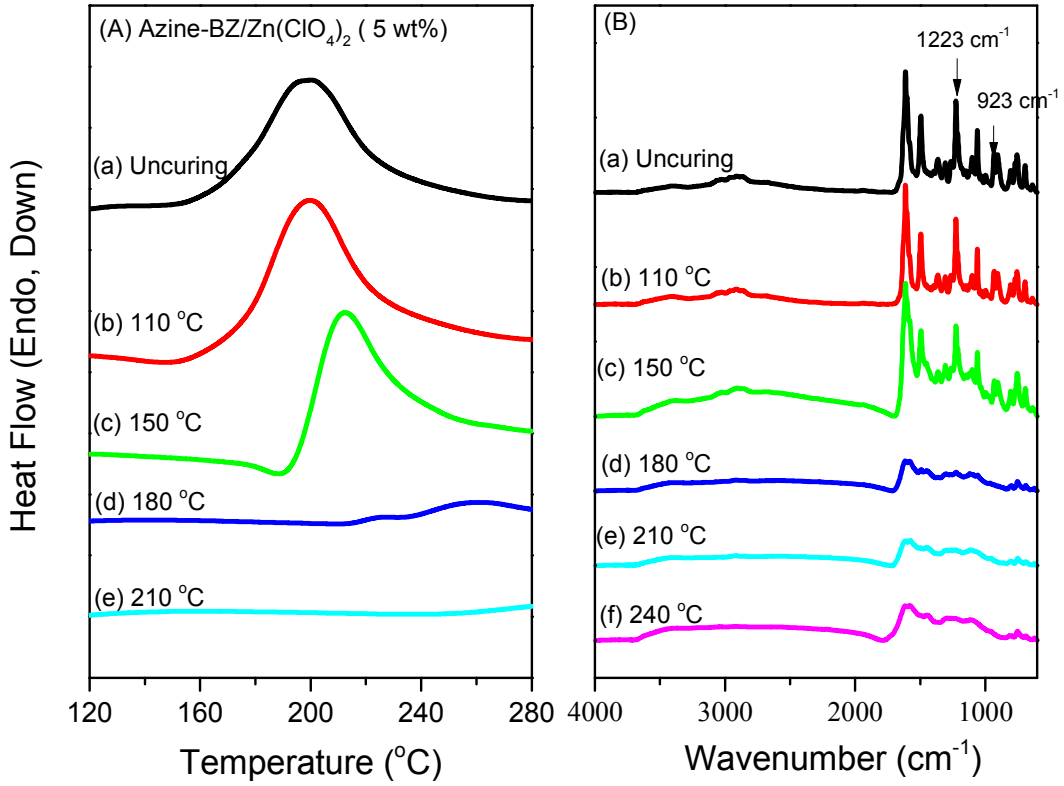

Figure 11: (A) DSC thermograms and (B) FTIR spectra of Azine-BZ monomer in the presence of 5 wt% $Zn(ClO_4)_2$, recorded after each curing stage

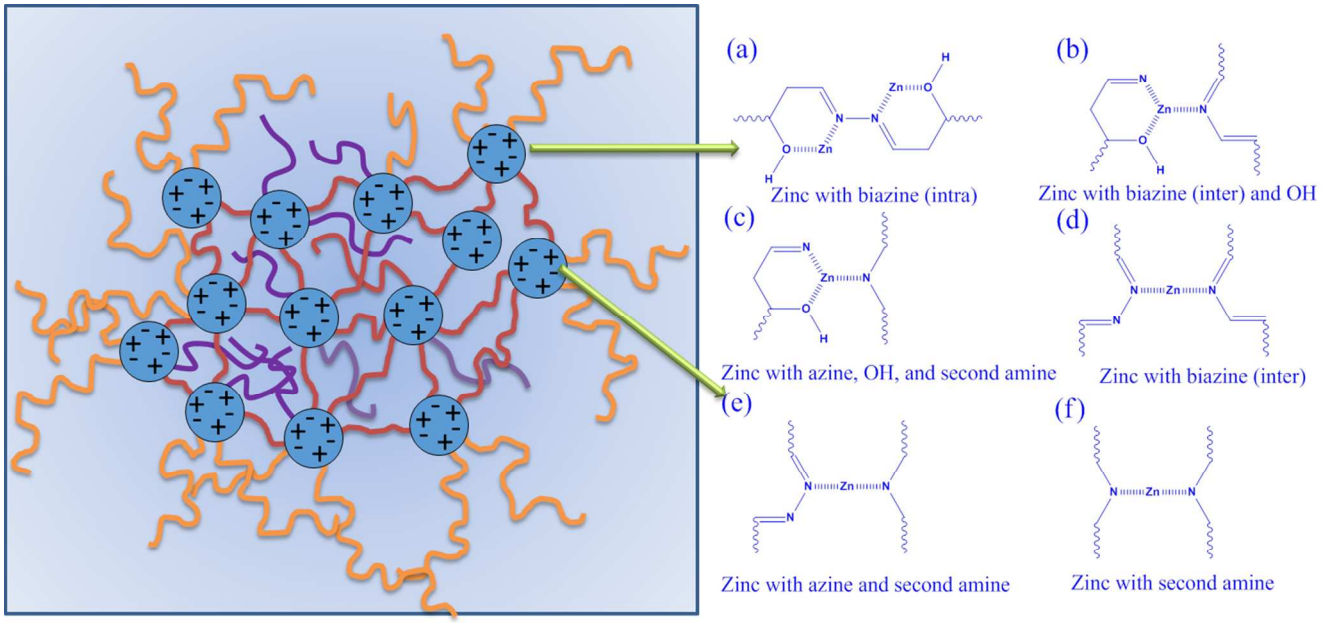

Scheme 2: (Left) Possible model of a poly(Azine-BZ)/$Zn(ClO_4)_2$ complex. (Right) Possible modes of metal–ligand complexes between $Zn(ClO_4)_2$ and poly(Azine-BZ).

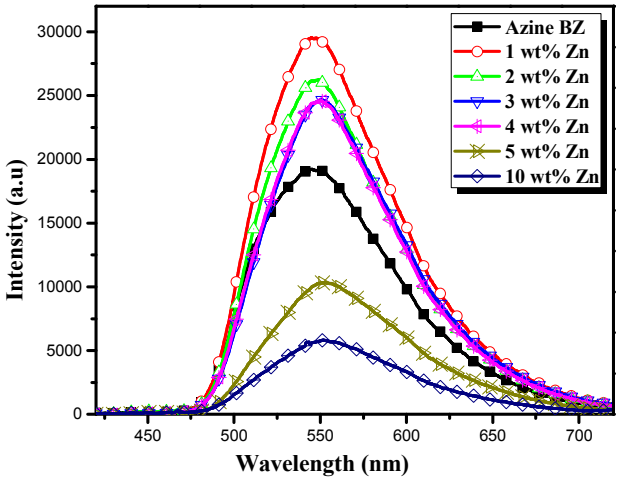

Figure 12: PL spectra of Azine-BZ blended with a various weight ratios of $Zn(ClO_4)_2$ in the bulk state, recorded at room temperature.

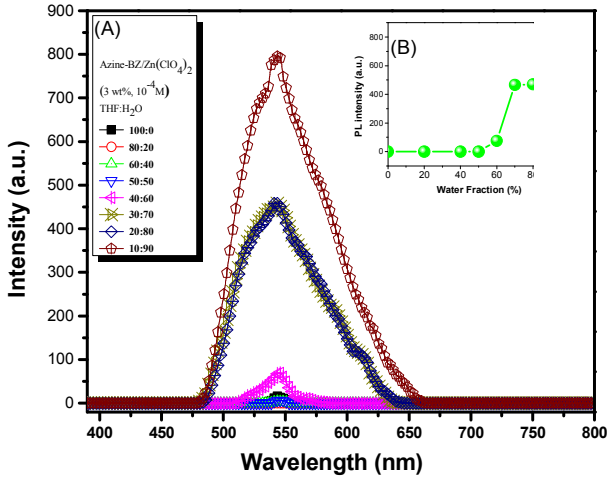

Figure 13: (A) PL spectral changes and (B) PL intensities of Azine-BZ blended with 3 wt% $Zn(ClO_4)_2$ (1.0×10^{-4} mol L^{-1}) in THF/water mixtures at various water fractions.

In addition, the thermal polymerization of Azine-BZ/5 wt% $Zn(ClO_4)_2$ complex was studied by DSC measurement. As revealed in Figure 11(A), the enthalpy of the curing exotherm decreased gradually upon increasing the temperature of the curing process, reaching zero at a curing temperature of 180 °C. Figure 11(B) presents corresponding FTIR spectra recorded after thermal curing of the 5 wt% $Zn(ClO_4)_2$ blend at various temperatures. The characteristic absorption bands of the ozaxine units at 1223 and 931 cm^{-1} disappeared after thermal curing at temperatures from 180 to 240 °C. Much literature reported there are many catalysts (e.g. Li^+, Fe^{+3}...) can act as effective promotors and accelerating for ring-opening polymerization of benzoxazine. The mechanism of ring-opening polymerization of benzoxazines using catalyst is divided into three steps; coordination-ring opening, electrophilic attack and finally rearrangement affording to phenolic and phenoxy structure.[42] We suspect that the Zn^{2+} ions coordinated effectively to the O and/or N atoms during ring opening of the BZ units; Scheme 2 presents some possible structures.

As mentioned above, the salicylaldehyde azine derivatives exhibit AIE features and emit light in their aggregated state because of restricted rotation of their N–N single bonds; in addition, salicylaldehyde azines bearing ortho OH groups on their phenyl rings can undergo intramolecular hydrogen bonding, which could lead to excited state intramolecular proton transfer (ESIPT). [33,43] Azine-BZ exhibits weak emission in solution because of intramolecular hydrogen bonding between the phenolic OH group and the N atom of the imino group that undergoes ESIPT phenomena. We were also interested in examining the AIE-active behavior of Azine-BZ when blended with $Zn(ClO_4)_2$. Figure 12 presents the PL spectra of Azine-BZ in the presence of various amounts of $Zn(ClO_4)_2$ in the bulk state. Interestingly, the PL intensities

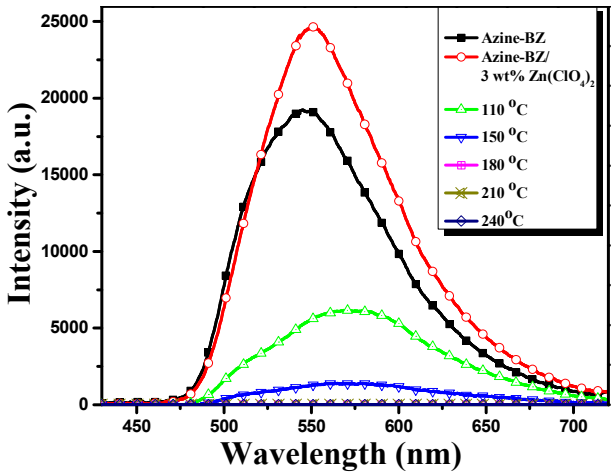

Figure 14: PL spectra of Azine-BZ blended with 3 wt% $Zn(ClO_4)_2$ in the bulk state, recorded at room temperature after each thermal curing stage

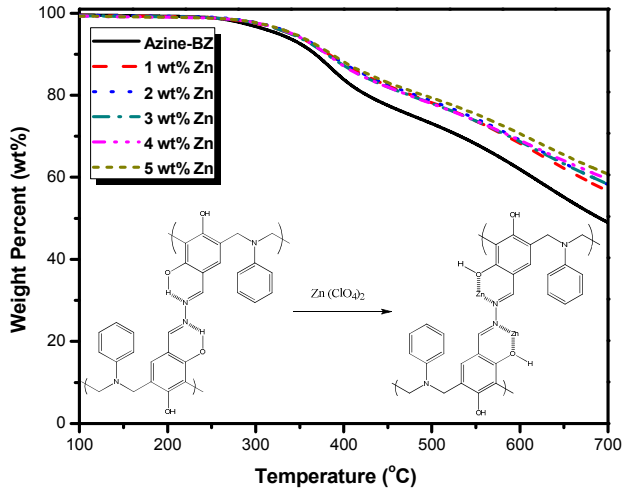

Figure 15: TGA analyses of Azine-BZ blended with various amounts of $Zn(ClO_4)_2$, recorded after thermal curing at 210 °C

when the contents of zinc ions were 1, 2, 3, and 4 wt% were higher than that of pure Azine-BZ, due to the Zn^{2+} ion having closed-shell *d*-orbitals; thus, the energy transfer process could not occur, leading to enhance metal–ligand charge transfer (MLCT),[36,37] as depicted in Scheme 2. In contrast, the PL intensity decreased when content of Zn^{2+} ions was 5 or 10 wt%, presumably because the Zn^{2+} ions coordinated to the azine units as displayed in Figure 10, changing the mechanism of the MLCT. To further study the optical properties of the aggregated Azine-BZ/3 wt% Zn^{2+} ion complex, we examined the fluorescence in THF in the presence of a poor solvent (water). As revealed in Figure 13, Azine-BZ in the presence of 3 wt% Zn^{2+} ions in pure THF displayed a non-emissive PL intensity, with the PL intensity increasing upon addition of water up to a fraction of 90%—characteristic AIE behavior. Figure 14 presents PL spectra of the Azine-BZ/3 wt% $Zn(ClO_4)_2$ complex after thermal curing at various temperatures. The PL intensity of this complex was higher than that of pure Azine-BZ prior to curing, consistent with MLCT. Upon increasing the curing temperature, the PL intensity decreased gradually until quenching completely at curing temperatures from 180 to 240 °C, similar to the behavior of the pure Azine-BZ monomer.

Figure 15 presents the thermal stability of Azine-BZ blended with various contents of $Zn(ClO_4)_2$ after thermal curing at 210 °C under N_2 at heating rate 20 °C/min, as investigated using TGA. As expected, the thermal decomposition temperature and char yield both increased upon increasing the $Zn(ClO_4)_2$ content. we found that the decomposition temperature value (Td_5) and char yield for the Azine-BZ/5 wt% Zn^{2+} complex was higher (350 °C, 61 wt%) than that for pure Azine-BZ (312 °C, 48 wt%), because the Zn^{2+} ions increased the degree of crosslinking (inset to Figure 15), in addition to the crosslinking through intra- and intermolecular hydrogen bonding, after ring opening.

Conclusions

A new Azine-based BZ monomer has been designed and that exhibits aggregation induced emission (AIE) behavior. DSC analysis revealed that the exothermic peak for the ring opening polymerization of Azine-BZ shifted to lower temperature, compare to that for a standard BZ, because the basicity of the phenolic unit facilitated the ring opening process. Furthermore, the azine unit in the BZ monomer has high affinity for Zn^{2+} ions, not only promoting ring opening polymerization at a lower curing temperature (from 213 °C in the absence of the Zn^{2+} ions to 184 °C in their presence). Based on thermogravametric results, the improving of thermal stability of Azine-BZ/$Zn(ClO_4)_2$ complexes, due to the presence of strong polymer-metal complexes. Azine-BZ coordinated with $[Zn(ClO_4)_2]$ through metal–ligand interactions, increasing the fluorescence emission intensity relative to that of the pure Azine-BZ monomer as a result of MLCT. The PL properties of the azine units and the metal–ligand complexes mode suggest that such monomers might be act as probes for realizing the thermal curing behavior of BZ rings; as fluorescent chemosensors for Zn^{2+} and other transition metal ions, even at high curing temperatures (e.g., 150 °C); and as components within polymer/inorganic hybrid materials.

Acknowledgment

This study was supported financially by the Ministry of Science and Technology, Taiwan, Republic of China, under contracts MOST103-2221-E-110-079-MY3 and MOST102-2221-E-110-008-MY3. We thank Mr. Hsien-Tsan Lin of the Regional Instruments Center at National Sun Yat-Sen University for help with the TEM experiments.

Electronic Supplementary Information (ESI) Available: FTIR, UV, MS, and ^1H NMR spectra of pure Azine-BZ.

References

(1) H. Ishida, "Handbook of Polybenzoxazine", ed. Ishida, H. and Agag, T., Elsevier, Amsterdam 2011, ch. 1, p. 1.
(2) N. Ghosh. B. Kiskan and Y. Yagci , *Prog. Polym. Sci.,* 2007, **32**:1344-1391.
(3) Y. Yagci Y, B. Kiskan and N.N .Ghosh, *J. Polym. Sci. Part A: Polym. Chem.,* 2009, **47**, 5565-5576.
(4) (a) T. Takeichi and T. Agag, *High Perform. Polym*., 2006, **18**, 777-797. (b) Y. X. Wang and H. Ishida, *Polymer*, 1999, **40**, 4563-4570. (c) M. Zhang, Z. Tan, S. Hu, J. Qiu and C. Liu, *RSC. Adv*., 2104, **4**, 44234-44243.
(5) (a) H. Ishida and Y. H. Lee, *Polym. Polym. Compos*., 2011, **9**, 121-134. (b) H. D. Kim and H. Ishida, *J. Phys. Chem. A*., 2002, **106**, 3271-3280. (c) H. D. Kim and H. Ishida, *Macromol. Symp*., 2003, **195**, 123-140. (d) S. W. Kuo, Y. C. Wu, C. F. Wang and K. U. Jeong, *J. Phys.*

Chem. C., 2009, **13**, 20666-20673. (e) C. F. Wang, S. F. Chiou, F. H. Ko, J. K. Chen, C. T. Chou, C. F. Huang, S. W. Kuo and F. C. Chang, *Langmuir.*, 2007, **23**, 5868-5871. (f) W. H. Hu, K. W. Huang, and S. W. Kuo, *Polym. Chem.,* 2012, **3**, 1546-1554.

(6) (a) Q. Li, and X. Zhong, *Langmuir,* 2007, **27**, 8365-8369. (b) H. Oie, A. Sudo and T. Endo, *J. Polym. Sci., Part A: Polym. Chem*., 2011, **49**, 3174-3183. (c) A. Sudo, R. Kudo, H. Nakuyama, K. Airma and T. Endo, *Macromolecules*, 2008, **41**, 9030-9034. (d) S. W. Kuo and F. C. Chang, *Prog. Polym. Sci*., 2011, **36**, 1649-1696. (e) M. G. Mohamed, K. C. Hsu, and S. W. Kuo, *Polym. Chem.,* 2015, **6**, 2423-2433. (f) C. Li, Q. Ran, R. Zhu, and Y. Gu, *RSC Adv.*, 2015, **5**, 22593-22600.

(7) C. K. Chozhan, M. Alagar and P. Gnanasundarm, *Acta Mater*., 2009, **28**, 338-794.

(8) M. G. Mohamed, H. K. Shih, and S. W. Kuo, *RSC Adv.,* 2015, **5**, 12763-12772.

(9) H. Ishida and H. Y. Low, *Macromolecules*, 1997, **30**, 1099-1106.

(10) T. Agag and T. Takeichi, *Polymer*, 2000, **41**, 7083-7090.

(11) P. Phirivawirut, R. Magaraphan and H. Ishida, *Mater. Res. Innova*., 2001, **4**, 187-198.

(12) M. R. Vengatesan, S. Devaraiu , K. Dinkaran and M. Alagar, *J. Mater. Chem.,* 2012, **22**, 7559-7559.

(13) C. F. Wang, Y. C. Su, S.W. Kuo, C.F. Huang, Y. C. Sheen and F. C. Chang, *Angew. Chem. Int. Ed.,* 2006, **45**, 2248-2251.

(14) T. Agag, R. C. Arza, F. H. J. Maurer and H. Ishida, *Macromolecules*, 2010, **43**, 2748-2758.

(15) A. Chernykh, T. Agag and H. Ishida, *Polymer*, 2009, **50**, 3153-3157.

(16) H. M. Qi, G. Y. Pan and Q. Y. Zhuang, *Polym. Eng. Sci.,* 2010, **50**, 1751-1757.

(17) Z. Brunovska, and H. Ishida, *J. Appl. Polym. Sci*., 1999, **73**, 2937-2949.

(18) T. Takeichi, K. Nakamura, T. Agag and H. Muto, *Des. Monomers Polym*., 2004, **7**, 727-740.

(19) R. Kudoh, A. Sudo and T. Endo, *Macromolecules*, 2010, **43**, 1185-1187.

(20) Y. C. Ye, Y. J. Huang, F. C. Chang, Z. G. Xue and X. L. Xie, *Polym. Chem*., 2014, **5**, 2863-2871.

(21) (a) J. Liu, C. Scott, S. Winroth, J. Maia, and H. Ishida, *RSC Adv*., 2015, **5**, 16785-16791. (b) K. Sethuraman, and M. Alagar, *RSC Adv.,* 215, **5**, 9607-9617. (c) R. Sasikumar, M. Ariraman, M. and M. Alagar, *RSC Adv.*, 2014, **4**, 19127-19136.

(22) S. W. Thomass, G. D. Joly and T. M. Swager, *Chem. Rev*., 2007, **107**, 1339-1386.

(23) C. T. Chen, *Chem. Mater*., 2004, **16**, 4389-4400.

(24) R. T. K. Kwok, J. L. Geong, J. W. Y. Lam, E. G. Zhao, G. Wang, R. Y. Zhan, B. Liu and B. Z. Tang, *J. Mater. Chem. B*., 2014, **2**, 4134.

(25) Y. Q. Dong, J. W. Y. Lam, A. J. Qin, Z. Li, J. Z. Sun, H. Y. Sung, I. D. Williams and B. Z. Tang, *Chem. Commun*., 2007, 40-42.

(26) H. Saigusa and E. C. Lim, *J. Phys. Chem*., 1995, **99**, 15738-15747.

(27) J. Luo, Z. Xie, J. W. Y. Lam, L. Cheng, H. Chen, C. Qiu, H. S. Kwok, X. Zhan, Y. Liu, D. Zhu and B. Z. Tang, *Chem. Commun*., 2001, 1740-1741.

(28) J. Chen, C. C. W. Law, J. W. Y. Lam, Y. Dong, S. M. F. Lo, I. D. Williams, D. Zhu and B. Z. Tang, *Chem. Mater*., 2003, **15**, 1535-1546.

(29) Y. P. Li, F. Li, H. Y. Zhang, Z. Q. Xie, W. J. Xie, H. Xu, B. Li, F. Y. Z. Shen and L. M. Hanif, *Chem. Commun*., 2007, 231-233.

(30) Z. P. Yu, Y. Y. Duan, L. H. Cheng, Z. L. Han, Z. Zheng, H. P. Zhou, J. Y. Wu and Y. P. Tian, *J. Mater. Chem*., 2012, **22**, 16927-16932.

(31) Y. Qian, M. M. Cai, X. H. Zhou, Z. Q. Gao, X. P. Wang, Y. Z. Zhao, X. H. Yan, W. Wei, L. H. Xie and W. Huang, *J. Phys. Chem. C*, 2012, **116**, 12187-12195.

(32) Z. Q. Xie, B. Yang, G. Cheng, L. L. Liu, F. He, F. Z. Shen, Y. G. Ma and S. Y. Liu, *Chem. Mater.*, 2005, **17**, 1287-1289.

(33) W. Tang, Y. Xiang and A. Tong, *J. Org. Chem*., 2009, **74**, 2163-2166.

(34) S. L. Liu, D. Li, Z. Zhang, G. K. S. Prakash, P. S. Conti, Z. B. Li, *Chem. Commun*., 2014, **50**, 7371.

(35) L. L. Long, W. Y. Lin, B. B. Chen, W. S. Gao, L. Yuan, *Chem. Commun*., 2011, **47**, 893.

(36) B. K. An, S. K. Kwon, S. D. Jung, S. Y. Park, *J. Am. Chem. Soc*., 2002, **124**, 14410-14415.

(37) W. Tang, Y. Xiang and A. Tong, *J. Org. Chem.*, 2009, **74**, 2163-2166.

(38) G. Liu, M. Yang, L. Wang, J. Zheng, H. Zhou, J. Wu and Y. Tian, *J. Mater. Chem. C.,* 2014, **2**, 2684-2691.

(39) M. G. Mohamed, W. C. Su, Y. C. Lin, C. F. Wang, J. K. Chen, K. U. Jeong and S. W. Kuo, *RSC Adv.*, 2014, **4**, 50373-50385.

(40) Y. H. Low and H. Ishida, *Polym. Degrad. Stab.*, 2006, **91**, 805-815.

(41) O. T. Lekesiz and J. Hacaloglu, *Polymer*, 2014, **55**, 3533-3542.

(42) C. Liu, D. Shen, M. R. Sebastian, J. Marquet and R. Schonfold, *Macromolecules*, 2011, **44**, 4616-4622.

(43) T. S. Hsiao, S. L. Deng, K. Y. Shih and J. L. Hong, *J. Mater. Chem. C*, 2014, **2**, 4828-4834.

Graphical abstract

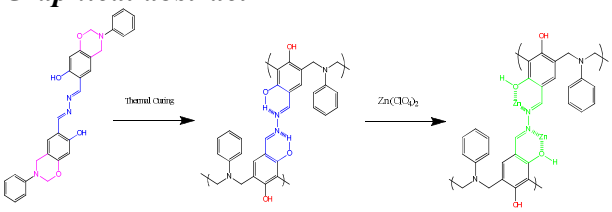

A new salicylaldehyde azine–functionalized benzoxazine (Azine-BZ) monomer formed benzoxazine/zinc ion complexes that not only improved the thermal properties but also facilitated ring-opening polymerization.